BESSM 2023, Vol 7, No 1, 58-65
https://doi.org/10.54987/bessm.v7i1.904

BULLETIN OF ENVIRONMENTAL SCIENCE & SUSTAINABLE MANAGEMENT

Website: http://journal.hibiscuspublisher.com/index.php/BESSM/index

Isothermal Modelling of the Adsorption of Malachite Green onto Rice husks

Bilal Ibrahim Dan-Iya[1], Salihu Yahuza[2], Ibrahim Alhaji Sabo[3], Abdullahi Adamu Faggo[4] and Mohd Ezuan Khayat[1,5]*

[1]Department of Biochemistry, Faculty of Biotechnology and Biomolecular Sciences, Universiti Putra Malaysia, 43400 UPM Serdang, Selangor, Malaysia.
[2]Department of Microbiology and Biotechnology, Faculty of Science, Federal University Dutse, PMB 7156, Dutse, Jigawa State, Nigeria.
[3]Department of Microbiology, Faculty of Science, Bauchi State University Gadau, P.M.B 065, Bauchi, Nigeria., PMB 065, Nigeria.
[4]Department of Microbiology, Faculty of Pure and Applied Sciences, Federal University Wukari, Taraba state, Nigeria.
[5]Agribiotechnology Group, Faculty of Biotechnology and Biomolecular Sciences, Universiti Putra Malaysia, UPM 43400 Serdang, Selangor, Malaysia.

*Corresponding author:
Mohd Ezuan Khayat,
Department of Biochemistry,
Faculty of Biotechnology and Biomolecular Sciences,
Universiti Putra Malaysia,
43400 UPM Serdang,
Selangor,
Malaysia.
Email: m_ezuan@upm.edu.my

HISTORY

Received: 15th April 2023
Received in revised form: 23rd June 2023
Accepted: 19th July 2023

KEYWORDS

Biosorption
Malachite Green
Isotherm
Modified rice husks
Jovanovic isotherm

ABSTRACT

The rice milling process produces rice husks as a by-product. It is one of the most important agricultural leftovers in terms of volume. The data of the sorption isotherm of Malachite Green sorption onto rice husks, which was plotted using linearized plots of isothermal models were reanalyzed using twenty isothermal models using nonlinear regression. Nineteen models — Henry, Langmuir, Freundlich, Jovanovic, Redlich-Peterson, Sips, Toth, Hill, Khan, BET, Vieth-Sladek, Radke-Prausnitz, Fritz-Schlunder III, Unilan, Baudu, Marczewski-Jaroniec, Fritz-Schluender IV, Weber-van Vliet and Fritz-Schluender V – fitted the data best using non-linear regression. Statistical analysis based on error function analyses such as root-mean-square error (RMSE), adjusted coefficient of determination (adjR^2), accuracy factor (AF), bias factor (BF), Bayesian Information Criterion (BIC), corrected AICc (Akaike Information Criterion), and Hannan-Quinn Criterion (HQC) showed that the best isotherm model was found to be the Redlich-Petersen with the lowest RMSE and AF, BF and adjR2 values closest to unity and lowest BIC, HQC and AICc values followed (descending order) by Jovanovic, Langmuir, Henry and Freundlich. The maximal adsorption capacity in the Jovanovic model will be used for comparative purposes since the Redlich-Petersen model does not feature a similar parameter. The maximal adsorption capacity expressed in milligrams per gram (mg/g), for the Jovanovic model, denoted by q_{mJ} and K_J-the Jovanovic constant, showed the calculated values of 4.04 mg/L (95% confidence interval; 3.306 to 4.773) and 0.445 (95% confidence interval; 0.264 to 0.627), respectively. The nonlinear regression method provides parameter values within the 95% confidence interval, facilitating improved comparability with prior research.

INTRODUCTION

Dyes are of major importance in almost all developing countries because dyes add color to textiles, paper, leather, and other materials to beautify and preserve them, and dyes are also a major concern because of the environmental pollution and health concerns of dye contamination [1]. A dye is a powdered material that is mixed with another product or dissolved in a liquid (like paint or ink). Pigments are dispersed solids that are often powdered [2]. The aesthetic and protective properties of both natural and synthetic dyes have led to their widespread use. Natural colors used to be simple to separate from their complicated mixes, but now the process is infamously difficult and time-consuming. The creation of contemporary synthetic dyes may also be traced back to these colors. Because of their conjugated structure, chromophores, and absorbing chromophores, dyes are exceptional among organic compounds in their ability to absorb light in the visible range [3]. It is a significant difficulty to remove colours from wastewater using conventional treatment methods. Fish and other aquatic species

https://doi.org/10.54987/bessm.v7i1.904

are in danger from the toxic organic compounds found in the wastewater dumped into rivers from dye manufacturing and textile finishing industries [4]. Many industries rely on colorants, including those dealing with textiles, paper, and plastics. Large volumes of noxious, discolored effluent byproducts are produced and eventually make their way into water supplies [3]. Whether on purpose or by mistake, technical developments in industry have contributed to the increase in pollution that has accompanied the growth of cities and their inhabitants. Textile businesses must process their effluents prior releasing them into the environment to prevent the emission of industrial waste effluents [5]. The contamination of water supplies with molecules of synthetic colors has detrimental impacts on both ecosystems and human health.

Dye runoff is a form of aesthetic pollution that causes to eutrophication. Dyeing textiles, leather, paper, paint, acrylic, cosmetics, polymers, and medicines is crucial to modern life. A lot of water is consumed by them as well [6]. This produces large amounts of muddy effluent. Because of the possible dangers associated with color pollution in drinking water, this study was conducted.

Dye removal is a prerequisite for discharging wastewater. Alternatives to physical diversion include chemical oxidation with chlorine and ozone and adsorption with alum, lime, ferric sulfate, and ferric chloride [7,8], membrane separation processes [9,10], and adsorption [9,10]. Adsorption-based treatments have shown the most promise. Adsorption and electrochemical coagulation are only two examples of the growing popularity of physicochemical techniques. Adsorption's increased popularity can be attributed to the many uses it can serve [11,12].
However, the idea that absorbed therapeutants may also have major internal effects was not taken into account when malachite green was widely utilized as a topical therapy in the aquaculture industry using bath or flush procedures. In addition to its uses as a food coloring agent, medical disinfectant, food additive, and anthelminthic, it is also put to use as a dye in the production of silk, wool, paper,, cotton, jute, leather and acrylic

Malachite Green (MG), a component of the triphenylmethane dye family, has several uses outside of the textile industry, including those of a fungicide and an ectoparasiticide in fisheries. Many fish species are believed to be harmful to humans at concentrations as low as 1 mg/L, and the effects of MG on aquatic organisms are intensively being studied. However, the dye and its metabolites are known to accumulate in aquaculture products such fish, prawn, and crab. It may be harmful to human health since it is carcinogenic and genotoxic [13–16]. Leucomalachite green, a reduced form of malachite green used to treat and prevent fungal and parasitic infections, builds up in the tissues of exposed fish. Serum, kidney, liver, skin, muscle, and viscera of a wide range of experimental animals, including fish, are the primary storage sites for this protein [17–19].

For this reason, its usage has been outlawed in a number of nations. The United States of America, the European Union, and others fall under this category. Because of its great efficiency, low cost, and widespread availability, MG is still in use in several regions of the world. The ease with which it may be obtained raises concerns that it will be misused. In the US, it is used to cure diseases in tropical fish. The use of MG to treat external parasites and fungal diseases in fish farming has been prevalent in Asian countries. However, MG removal from aquaculture wastewater has been largely overlooked in comparison to the elimination of other pollutants.

Consequences for the ecology may result from MG pollution in aquaculture wastewater [20–23]. There are various distinct types of malachite green on the marketplace, the most prevalent of which being a fifty % solution of the hydrochloride or oxalate salt. Industrial grade malachite green hydrochloride is precipitated as a double zinc salt with the introduction of zinc chloride during manufacturing. This dye, like other triphenylemethanes, may exist as the dye salt as well as the carbinol or pseudobase ionic forms. These ions are more ready to enter cells as the pseudobase because of its high lipid solubility [24].

The adsorption process can only be understood in this setting if the kinetics and isotherms are correctly assigned. It is common practice in the literature to portray the plainly nonlinear curve in this data in a linearized manner. When nonlinear data is linearized, the error structure of the data shifts, making it more difficult to estimate uncertainty [25]. In this investigation, we fit several isothermal models to previously reported data on MG adsorption onto rice husks and performed a nonlinear regression analysis. In order to determine the isotherm that best fits the data, numerous error function studies were performed.

METHOD

Data acquisition and fitting

Figure 10 data from a previously published study [26] was digitized using the freeware Webplotdigitizer 2.5 [27]. After that, Curve-Expert Professional, a curve-fitting application, was used to do a nonlinear regression on the data (Version 1.6). This software's reliability in conducting digital conversions has been lauded and showed excellent agreement to original data [28,29].

Table 1. Mathematical isothermal models that were utilized in modelling data [30,31].

Isotherm	p	Formula	Ref.
Henry's law	1	$q_e = HC_e$	[32]
Langmuir	2	$q_e = \frac{q_{mL} b_L C_e}{1 + b_L C_e}$	[30]
Jovanovic	2	$q_e = q_{mJ}(1 - e^{-K_j C_e})$	[33]
Freundlich	2	$q_e = K_F C_e^{\frac{1}{n_F}}$	[34]
Temkin	3	$q_e = \frac{RT}{b_T}\{ln(a_T C_e)\}$	[35]
Dubinin-Radushkevich	2	$q_e = q_{mDR} exp\left\{-K_{DR}\left[RT ln\left(1 + \frac{1}{C_e}\right)\right]^2\right\}$	[36,37]
Redlich-Peterson	3	$q_e = \frac{K_{RP1} C_e}{1 + K_{RP2} C_e^{\beta_{RP}}}$	[38]
Sips	3	$q_e = \frac{K_S q_{mS} C_e^{\frac{1}{n_S}}}{1 + K_S C_e^{\frac{1}{n_S}}}$	[39]
Toth	3	$q_e = \frac{q_{mT} C_e}{\left(K_T + C_e^{n_T}\right)^{n_T}}$	[40]
Hill	3	$q_e = \frac{q_{mH} C_e^{n_H}}{K_H + C_e^{n_H}}$	[9]
Khan	3	$q_e = \frac{q_{mK} b_K C_e}{(1 + b_K C_e)^{a_K}}$	[41]
BET	3	$q_e = \frac{q_{mBET} \alpha_{BET} C_e}{(1 - \beta_{BET} C_e)(1 - \beta_{BET} C_e + \alpha_{BET} C_e)}$	[42]
Vieth-Sladek	3	$q_e = \frac{q_{mVS} b_{VS} C_e}{(1 + b_{VS} C_e)^{n_{VS}}}$	[43]
Radke-Prausnitz	3	$q_e = \frac{q_{mRP} K_{RP} C_e}{(1 + K_{RP} C_e)^{n_{RP}}}$	[44]
Brouers–Sotolongo	3	$q_e = q_{mBS}\left(-K_{BS} C_e^{n_{BS}}\right)$	[45]
Fritz-Schlunder-III	3	$q_e = \frac{q_{mFS} K_{FS} C_e}{1 + K_{FS} C_e^{n_{FS}}}$	[46]
Unilan	3	$q_e = \frac{q_{mU}}{2b_U} ln\left(\frac{a_U + C_e e^{b_U}}{a_U + C_e e^{-b_U}}\right)$	[15]

Statistical analysis

A set of statistical discriminatory tests such as corrected AICc (Akaike Information Criterion), Bayesian Information Criterion (BIC), Hannan and Quinn's Criterion (HQ), Root-Mean-Square Error (RMSE), bias factor (BF), accuracy factor (AF) and adjusted coefficient of determination (R^2) were used in this study.

The RMSE was computed using Equation 1, and it stands to reason that the fewer parameters utilized, the smaller the RMSE will be. n is for the total number of observations made in the experiment, Obi and Pdi stand for the total number of observations made in the experiment and projections, and p stands for the total number of parameters [25] .

$$RMSE = \sqrt{\frac{\sum_{i=1}^{n}(Pd_i - Ob_i)^2}{n-p}} \quad \text{(Eqn. 1)}$$

Because R^2 or the coefficient of determination ignores the number of parameters in a model, the modified R^2 is used to overcome this limitation. The entire variance of the y-variable is given by $S^2{}_y$ in the equation (**Equations 2** and **3**), while RMS is the Residual Mean Square.

$$Bias\ factor = 10\left(\sum_{i=1}^{n} log\frac{(Pd_i/Ob_i)}{n}\right) \quad \text{(Eqn. 2)}$$

$$Accuracy\ factor = 10\left(\sum_{i=1}^{n} log\frac{|(Pd_i/Ob_i)|}{n}\right) \quad \text{(Eqn. 3)}$$

The AICc is computed as follows (**Equation 4**), where p represents the number of parameters and n represents the number of data points. The corrected Akaike information criterion (AICc) is used to manage data with a large number of parameters but a limited number of values [47]. A model with a lower AICc score is considered more likely to be right [47]. The information theory is the foundation of the Akaike Information Criterion (AIC). It strikes a compromise between the goodness of fit of a given model and the model's complexity [48].

$$AICc = 2p + n\ln\left(\frac{RSS}{n}\right) + \frac{2(p+1)+2(p+2)}{n-p-2} \quad \text{(Eqn. 4)}$$

Another statistical tool based on information theory apart from AICc, is the Bayesian Information Criterion (BIC) (Equation 5). The number of parameters is penalized more severely by this error function than by AIC [27].

$$BIC = n\ln\left(\frac{RSS}{n}\right) + k\ln(n) \quad \text{(Eqn. 5)}$$

The Hannan-Quinn information criterion (HQC) (**Equation 6**) is another error function approach based on information theory. Because of the ln ln n element in the calculation, the HQC is more consistent than the AIC [47].

$$HQC = nln\left(\frac{RSS}{n}\right) + 2k\ln(\ln n) \quad \text{(Eqn. 6)}$$

The Accuracy Factor (AF) and Bias Factor (BF) are two further error function analyses derived from Ross's work [47]. These error functions evaluate models statistically for goodness-of-fit but do not penalize for the number of parameters (**Equations 7** and **8**).

$$Adjusted\ (R^2) = 1 - \frac{RMS}{S_Y^2} \quad \text{(Eqn. 4)}$$

$$Adjusted\ (R^2) = 1 - \frac{(1-R^2)(n-1)}{(n-p-1)} \quad \text{(Eqn. 5)}$$

RESULTS AND DISCUSSION

The equilibrium data from [26] was analyzed using seventeen one to three-parameter models (**Table 1**) by utilizing non-linear regression. As the datapoints are small, higher parameter models are excluded. Of these models, only Temkin and Dubinin-Radushkevich did not fit well with the data (**Figs. 1 – 15**).

The best isotherm model was found to be the Redlich-Petersen with the lowest RMSE and AF, BF and adjR^2 values closest to unity and lowest BIC, HQC and AICc values followed (descending order) by Jovanovic, Langmuir, Henry and Freundlich (**Table 2**). As enough models fitted well with the rice husks data, it explains and justifies the more accuracy of using nonlinear regression as against the linear regression used in the original publication which suggests the 2-parameter Jovanovic isotherm as the best model.

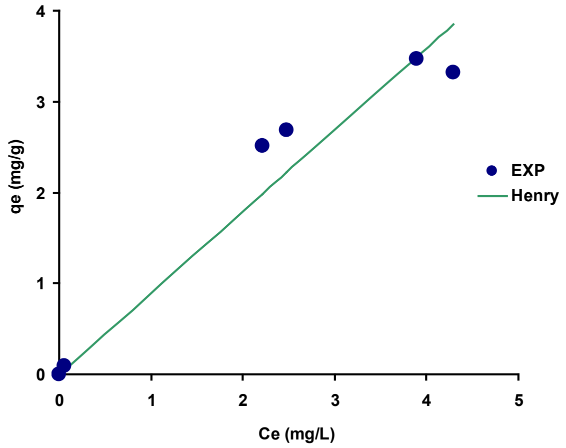

Fig. 1. Adsorption isotherm of Malachite Green onto rice husks as modelled using the Henry model.

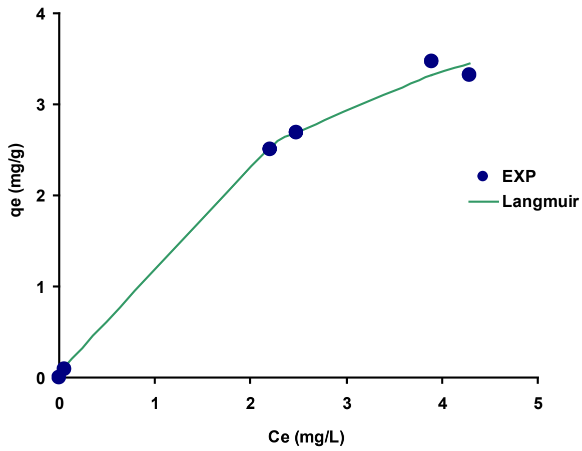

Fig. 2. Adsorption isotherm of Malachite Green onto rice husks as modelled using the Langmuir isotherm model.

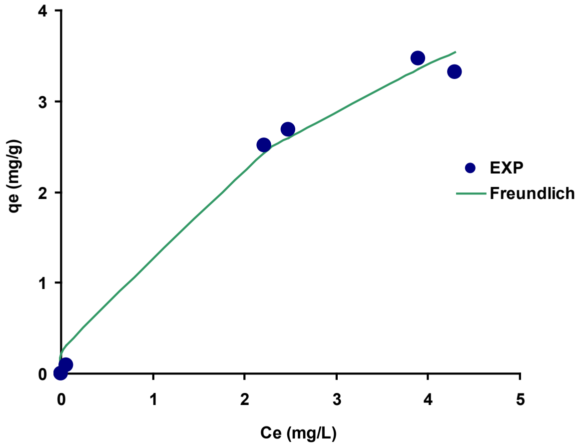

Fig. 3. Adsorption isotherm of Malachite Green onto rice husks as modelled using the Freundlich isotherm model.

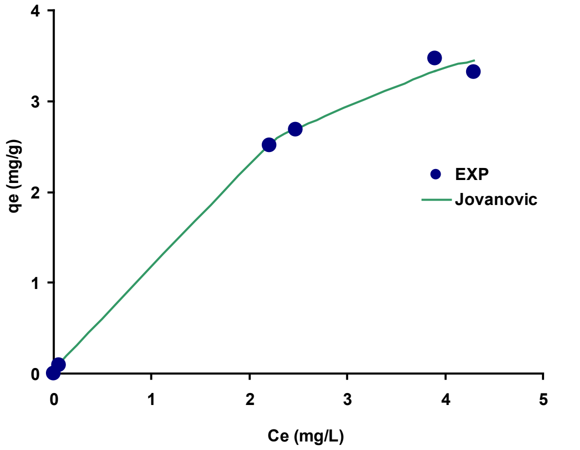

Fig. 4. Adsorption isotherm of Malachite Green onto rice husks as modelled using the Jovanovic isotherm model.

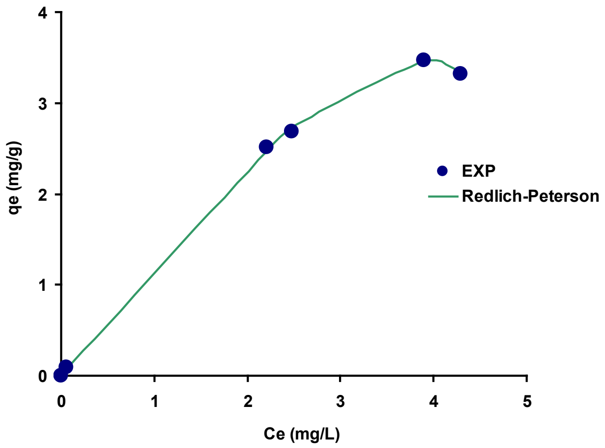

Fig. 5. Adsorption isotherm of Malachite Green onto rice husks as modelled using the Redlich-Peterson isotherm model.

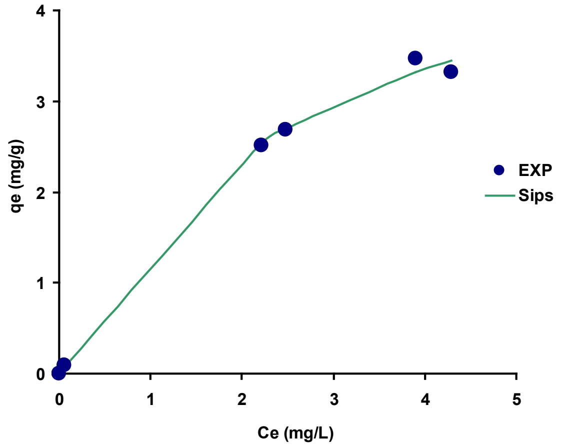

Fig. 6. Adsorption isotherm of Malachite Green onto rice husks as modelled using the Sips isotherm model.

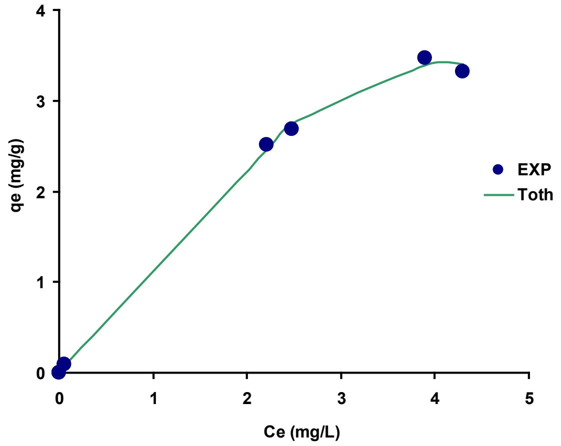

Fig. 7. Adsorption isotherm of Malachite Green onto rice husks as modelled using the Toth isotherm model.

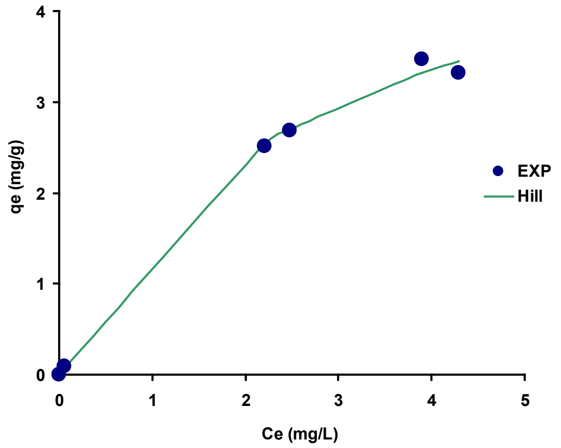

Fig. 8. Adsorption isotherm of Malachite Green onto rice husks as modelled using the Hill isotherm model.

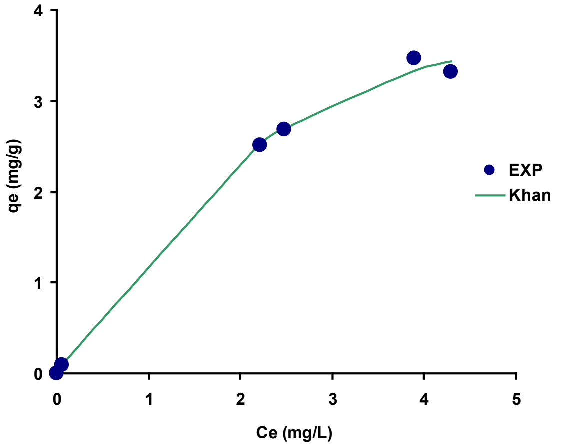

Fig. 9. Adsorption isotherm of Malachite Green onto rice husks as modelled using the Khan isotherm model.

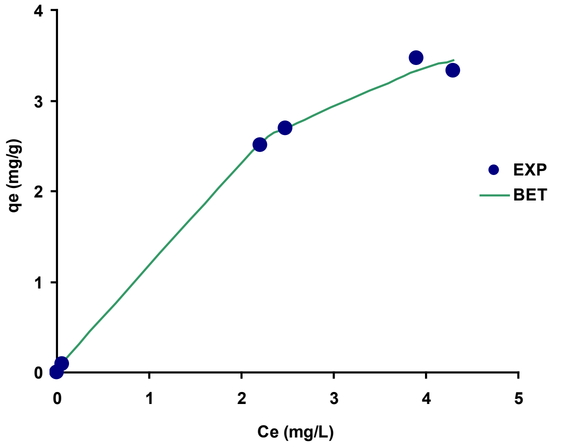

Fig. 10. Adsorption isotherm of Malachite Green onto rice husks as modelled using the BET isotherm model.

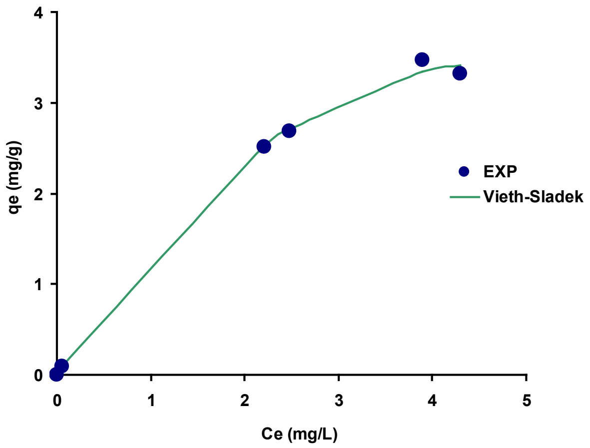

Fig. 11. Adsorption isotherm of Malachite Green onto rice husks as modelled using the Vieth-Sladek isotherm model.

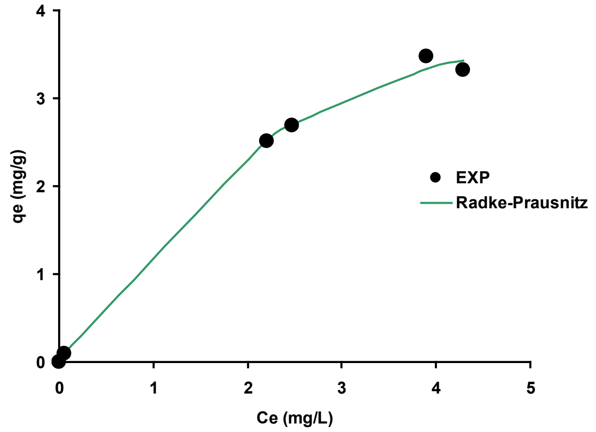

Fig. 12. Adsorption isotherm of Malachite Green onto rice husks as modelled using the Radke-Prausnitz isotherm model.

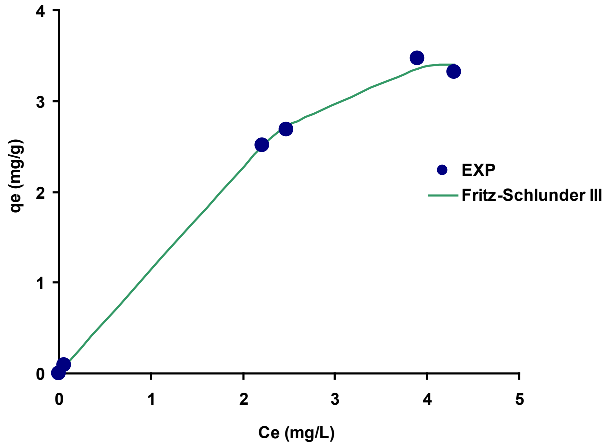

Fig. 13. Adsorption isotherm of Malachite Green onto rice husks as modelled using the Fritz-Schlunder III isotherm model.

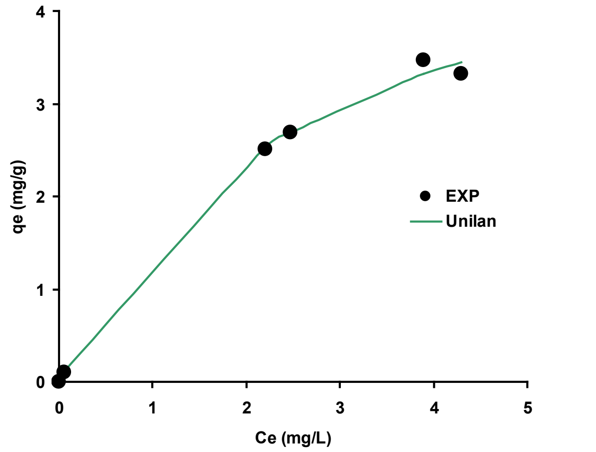

Fig. 14. Adsorption isotherm of Malachite Green onto rice husks as modelled using the Unilan isotherm model.

https://doi.org/10.54987/bessm.v7i1.904

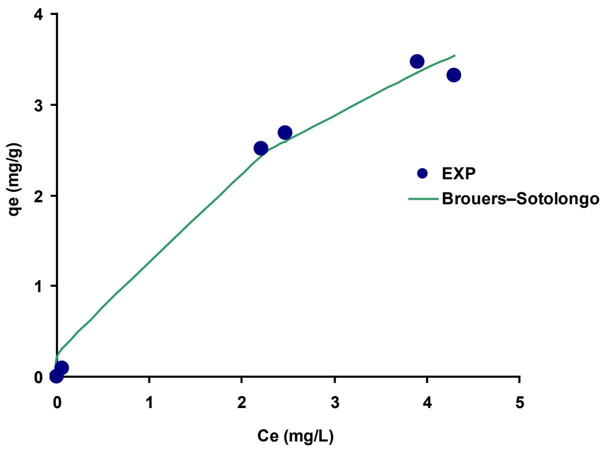

Fig. 15. Adsorption isotherm of Malachite Green onto rice husks as modelled using the Brouers–Sotolongo isotherm model.

Table 2. Error function analysis for the fitting of the isotherm of Malachite Green onto rice husks.

Model	p	RMSE	adR2	AICc	BIC	HQC	BF	AF
Henry	1	0.394	0.93	-2.27	-2.27	-10.47	0.86	1.22
Langmuir	2	0.100	0.99	-8.01	-8.01	-26.42	1.03	1.05
Freundlich	2	0.174	0.98	-1.38	-1.38	-19.80	1.21	1.25
Temkin	2	n.a.	n.a.	n.a.	n.a.	n.a.	n.a.	n.a.
Dubinin-Radushkevich	2	n.a.	n.a.	n.a.	n.a.	n.a.	n.a.	n.a.
Jovanovic	2	0.095	1.00	-8.70	-8.70	-27.11	1.01	1.02
Redlich-Peterson	2	0.035	1.00	-20.49	-20.49	-38.91	0.94	1.08
Sips	3	0.114	0.99	23.73	23.73	-24.89	0.95	1.07
Toth	3	0.080	1.00	19.60	19.60	-29.03	0.93	1.09
Hill	3	0.114	0.99	23.73	23.73	-24.89	0.95	1.07
Khan	3	0.103	0.99	22.62	22.62	-26.01	1.00	1.02
BET	3	0.109	0.99	23.27	23.27	-25.35	1.01	1.03
Vieth-Sladek	3	0.093	0.99	21.29	21.29	-27.34	0.99	1.03
Radke-Prausnitz	3	0.104	0.99	22.62	22.62	-26.00	1.00	1.02
Brouers–Sotolongo	3	0.201	0.97	30.62	30.62	-18.01	1.21	1.25
Fritz-Schlunder III	3	0.083	1.00	19.96	19.96	-28.66	0.95	1.06
Unilan	3	0.116	0.99	24.01	24.01	-24.62	1.03	1.05

Note:
RMSE Root mean Square Error
adR^2 Adjusted Coefficient of determination
p no of parameters
AF Accuracy factor
BF Bias factor
BIC Bayesian Information Criterion
AICc Adjusted Akaike Information Criterion
HQC Hannan–Quinn information criterion

The Redlich – Peterson isotherm features of both the Freundlich and Langmuir isotherms are incorporated into the three-parameter model. This model is a mixture of the two, therefore the adsorption mechanism does not follow the rules of ideal monolayer adsorption [49]. Numerous applications exist for the Redlich-Peterson isotherm model, which includes homogeneous and heterogeneous systems. The equation is as follows [50]. Adsorption equilibrium is represented by a linear dependence on concentration, which holds true over a wide concentration range. This is because the numerator is based on the Langmuir isotherm model, which allows it to enter the Henry zone at infinite dilution [51]. As the isotherm does not permit the q_{max} feature needed for comparing efficiency of sorption, the q_{max} value for the next best model, which is the Jovanovic isotherm will be used instead.

The Jovanovic isotherm considers an adsorption surface assumption, which is similar to the Langmuir's. A second approximation for localized monolayer adsorption in the absence of lateral interactions corresponds to this scenario. The main distinction between this model and the Langmuir model is that the surface binding vibrations of an adsorbed species are considered [33]. The maximal adsorption capacity in the Jovanovic model, expressed in milligrams per gram (mg/g), is denoted by q_{mJ} while K_j is the Jovanovic constant, and the calculated values were 4.04 mg/L (95% confidence interval; 3.306 to 4.773) and 0.445 (95% confidence interval; 0.264 to 0.627), respectively (**Table 3**). The isotherm additionally considers the surface binding vibrations of the adsorbed species. A 3-parameter Jovanovic isotherm is also available and considers multilayer adsorption [33].

Table 3. Isothermal models' constants for the TB dye adsorption using *Pseudomonas* sp. strain MM02.

Model	p	Unit	Value	(95% confidence interval)
Langmuir	q_{mL}	mg g^{-1}	5.614	3.903 to 7.325
	b_L	L mg^{-1}	0.372	0.122 to 0.622
Jovanovic	q_{mJ}	mg g^{-1}	4.04	3.306 to 4.773
	K_J	dimensionless	0.445	0.264 to 0.627
Redlich – Peterson	K_{RP1}	L mg^{-1}	1.131	1.070 to 1.191
	β_{RP}	dimensionless	5.381	2.655 to 8.106
	K_{RP2}	L g^{-1}	0.0000	-0.001 to 0.001
Sips	q_{mS}	mg g^{-1}	4.993	0.155 to 9.831
	K_S	L g^{1}	0.408	0.010 to 0.807
	n_S	dimensionless	0.858	-0.330 to 2.046
Hill isotherm	q_{mH}	mg g^{-1}	4.993	0.155 to 9.831
	n_H	dimensionless	1.165	-0.447 to 2.777
	K_H	dimensionless	2.448	0.059 to 4.838

Note
*Isotherm with *ln* term should not be plotted using data that starts from the origin (0,0)
‡Isotherms having an RT term should be plotted using the temperature (Kelvin) studied

Different sorbents can be coated, chemically synthesized, or otherwise manufactured to remove dyes, effluents, and trace elements from wastewater [46–51]. The milling process produces rice husks as a byproduct. It is one among the largest agricultural byproducts by volume. Twenty percent of Egypt's rice harvest has been attributed to the production of this waste [52,53].500 million tons of rice would be produced annually in developing nations, with around 100 million tons of rice husks accessible for use. In addition to being burned in boilers in the rice business, rice husks have also been utilized to make blocks and panels for use in civil construction [53,54]. But there are so many more rice husks that may be used locally that waste management is becoming an issue. This material was chosen because it does not need regeneration, has a granular structure, is chemically stable, and can be produced cheaply.

CONCLUSION

Seventeen adsorption isotherm models with one to three parameters have been fitted to the adsorption of MG to rice husks using non-linear regression. Root-mean-square error (RMSE), adjusted coefficient of determination ($adjR^2$), bias factor (BF), accuracy factor (AF), bias information coefficient (BIC), and the corrected Akaike Information Criterion (AICc) all indicate that the showed that taking into account all of the criteria, the Redlich-Petersen model came out on top. Since the isotherm does not provide the q_{max} characteristic necessary for comparing sorption efficiency, the q_{max} value for the Jovanovic isotherm will be used instead. The nonlinear regression method provides parameter values in the 95% confidence interval, which improves comparability with previous research.

REFERENCES

1. Lellis B, Fávaro-Polonio CZ, Pamphile JA, Polonio JC. Effects of textile dyes on health and the environment and bioremediation potential of living organisms. Biotechnol Res Innov. 2019;3(2):275–90.

2. Hielscher K. Ultrasonic Milling and Dispersing Technology for Nano-Particles. MRS Online Proc Libr. 2012;1479(1):21–6.
3. Homagai PL, Poudel R, Poudel S, Bhattarai A. Adsorption and removal of crystal violet dye from aqueous solution by modified rice husk. Heliyon. 2022;8(4):e09261.
4. Zabłocka-Godlewska E, Przystaś W, Grabińska-Sota E. Possibilities of Obtaining from Highly Polluted Environments: New Bacterial Strains with a Significant Decolorization Potential of Different Synthetic Dyes. Water Air Soil Pollut. 2018;229(6).
5. Slama H Ben, Bouket AC, Pourhassan Z, Alenezi FN, Silini A, Cherif-Silini H, et al. Diversity of synthetic dyes from textile industries, discharge impacts and treatment methods. Appl Sci Switz. 2021;11(14):1–21.
6. Khattab TA, Abdelrahman MS, Rehan M. Textile dyeing industry: environmental impacts and remediation. Environ Sci Pollut Res. 2020;27(4):3803–18.
7. Thamaraiselvan C, Noel M. Membrane processes for dye wastewater treatment: Recent progress in fouling control. Crit Rev Environ Sci Technol. 2015;45(10):1007–40.
8. Brik M, Chamam B, Schöberl P, Braun R, Fuchs W. Effect of ozone, chlorine and hydrogen peroxide on the elimination of colour in treated textile wastewater by MBR. Water Sci Technol. 2004;49(4):299–303.
9. Sivalingam S, Sen S. Rice husk ash derived nanocrystalline ZSM-5 for highly efficient removal of a toxic textile dye. J Mater Res Technol. 2020;9(6):14853–64.
10. Mohanty K, Naidu JT, Meikap BC, Biswas MN. Removal of crystal violet from wastewater by activated carbons prepared from rice husk. Ind Eng Chem Res. 2006;45(14):5165–71.
11. Quansah JO, Hlaing T, Lyonga FN, Kyi PP, Hong SH, Lee CG, et al. Nascent rice husk as an adsorbent for removing cationic dyes from textile wastewater. Appl Sci Switz. 2020;10(10).
12. Persulfate B activated, Avramiotis E, Frontistis Z, Manariotis ID, Vakros J, Mantzavinos D. Oxidation of Sulfamethoxazole by Rice Husk. 2021;
13. Srivastava S, Sinha R, Roy D. Toxicological effects of malachite green. Aquat Toxicol. 2004;66(3):319–29.
14. Guerra-Lopez D, Daniels L, Rawat M. *Mycobacterium smegmatis* mc2 155 fbiC and MSMEG_2392 are involved in triphenylmethane dye decolorization and coenzyme F420 biosynthesis. Microbiology. 2007;153(8):2724–32.
15. Chowdhury S, Mishra R, Saha P, Kushwaha P. Adsorption thermodynamics, kinetics and isosteric heat of adsorption of malachite green onto chemically modified rice husk. Desalination. 2011;265(1–3):159–68.
16. Witek-Krowiak A. Analysis of influence of process conditions on kinetics of malachite green biosorption onto beech sawdust. Chem Eng J. 2011 Jul 15;171(3):976–85.
17. Poe RW, Wilson RP. Absorption of malachite green by channel catfish. Progress Fish Cult U S Fish Wildl Serv. 1983;228–9.
18. Roybal JE, Pfenning AP, Munns RK, Holland DC, Hurlbut JA, Long AR. Determination of malachite green and its metabolite, leucomalachite green, in catfish (Ictalurus punctatus) tissue by liquid chromatography with visible detection. J AOAC Int. 1995;78(2):453–7.
19. Doerge DR, Churchwell MI, Gehring TA, Pu YM, Plakas SM. Analysis of malachite green and metabolites in fish using liquid chromatography atmospheric pressure chemical ionization mass spectrometry. Rapid Commun Mass Spectrom RCM. 1998;12(21):1625–34.
20. Khattri SD, Singh MK. Colour removal from synthetic dye wastewater using a bioadsorbent. Water Air Soil Pollut. 2000;120(3–4):283–94.
21. Myung HK, Kim Y, Park HJ, Jong SL, Kwak SN, Jung WH, et al. Structural insight into bioremediation of triphenylmethane dyes by *Citrobacter* sp. triphenylmethane reductase. J Biol Chem. 2008;283(46):31981–90.
22. Lian Z, Wang J. Molecularly imprinted polymer for selective extraction of malachite green from seawater and seafood coupled with high-performance liquid chromatographic determination. Mar Pollut Bull. 2012 Dec 1;64(12):2656–62.
23. Dhananjaneyulu BV, Kumaraswamy K. Kinetic and thermodynamic studies on adsorption of malachite green from aqueous solution using mixed adsorbents (Rice husk and egg shell). Res J Pharm Technol. 2016;9(10):1671–6.
24. Albert A. Selective toxicity. The physico-chemical basis of therapy. [Internet]. 7th ed. London, U.K.: Chapman & Hall; 1985 [cited 2023 May 29]. Available from: https://www.cabdirect.org/cabdirect/abstract/19802704337
25. Motulsky HJ, Ransnas LA. Fitting curves to data using nonlinear regression: a practical and nonmathematical review. FASEB J. 1987;1(5):365–74.
26. Muinde VM, Onyari JM, Wamalwa B, Wabomba J, Nthumbi RM. Adsorption of Malachite Green from Aqueous Solutions onto Rice Husks: Kinetic and Equilibrium Studies. J Environ Prot. 2017 Mar 10;8(3):215–30.
27. Dan-Iya BI, Shukor MY. Isothermal Modelling of the Adsorption of Chromium onto Calcium Alginate Nanoparticles. J Environ Microbiol Toxicol. 2021;9(2):1–7.
28. Khare KS, Phelan FR. Quantitative Comparison of Atomistic Simulations with Experiment for a Cross-Linked Epoxy: A Specific Volume-Cooling Rate Analysis. Macromolecules. 2018;51(2):564–75.
29. Halmi MIE, Ku Ahamad KE, Shukor MY, Wasoh MH, Abdul Rachman AR, Sabullah MK, et al. Mathematical modelling of the degradation kinetics of Bacillus cereus grown on phenol. J Environ Bioremediation Toxicol. 2014;2(1):1–8.
30. Langmuir I. THE ADSORPTION OF GASES ON PLANE SURFACES OF GLASS, MICA AND PLATINUM. J Am Chem Soc. 1918;40(2):1361–402.
31. Schirmer W. Physical Chemistry of Surfaces. Z Für Phys Chem. 1999;210(1):134–5.
32. Ridha FN, Webley PA. Anomalous Henry's law behavior of nitrogen and carbon dioxide adsorption on alkali-exchanged chabazite zeolites. Sep Purif Technol. 2009;67(3):336–43.
33. Jovanović DS. Physical adsorption of gases - I: Isotherms for monolayer and multilayer adsorption. Kolloid-Z Amp Z Für Polym. 1969;235(1):1203–13.
34. Carmo AM, Hundal LS, Thompson ML. Sorption of hydrophobic organic compounds by soil materials: Application of unit equivalent Freundlich coefficients. Environ Sci Technol. 2000;34(20):4363–9.
35. Temkin MI, Pyzhev V. Kinetics of ammonia synthesis on promoted iron catalysts. Acta Physicochim USSR. 1940;12(3):327–56.
36. Radushkevich LV. Potential theory of sorption and structure of carbons. Zhurnal Fiz Khimii. 1949;23:1410–20.
37. Dubinin MM. Modern state of the theory of volume filling of micropore adsorbents during adsorption of gases and steams on carbon adsorbents. Zh Fiz Khim. 1965;39(6):1305–17.
38. Redlich O, Peterson DL. A Useful Adsorption Isotherm. Shell Dev Co Emeryv Calif. 1958;63:1024.
39. Sips R. On the structure of a catalyst surface. J Chem Phys. 1948;16(5):490–5.
40. Tóth J. Uniform interpretation of gas/solid adsorption. Adv Colloid Interface Sci. 1995;55(C):1–239.
41. Khan AA, Singh RP. Adsorption thermodynamics of carbofuran on Sn (IV) arsenosilicate in H+, Na+ and Ca2+ forms. Colloids Surf. 1987;24(1):33–42.
42. Brunauer S, Emmett PH, Teller E. Adsorption of Gases in Multimolecular Layers. J Am Chem Soc. 1938;60(2):309–19.
43. Vieth WR, Sladek KJ. A model for diffusion in a glassy polymer. J Colloid Sci. 1965;20(9):1014–33.
44. Radke CJ, Prausnitz JM. Adsorption of Organic Solutes from Dilute Aqueous Solution of Activated Carbon. J Am Chem Soc. 1972;11(4):445–51.
45. Gregg SJ, Sing KSW. Adsorption, surface area, and porosity. London: Academic Press; 1991. 328 p.
46. Fritz W, Schluender EU. Simultaneous adsorption equilibria of organic solutes in dilute aqueous solutions on activated carbon. Chem Eng Sci. 1974;29(5):1279–82.
47. Burnham KP, Anderson DR. Multimodel inference: Understanding AIC and BIC in model selection. Sociol Methods Res. 2004;33(2):261–304.
48. Akaike H. A New Look at the Statistical Model Identification. IEEE Trans Autom Control. 1974;19(6):716–23.
49. Redlich O, Peterson DL. A useful adsorption isotherm. J Phys Chem. 1959;63(6):1024.
50. Sivarajasekar N, Baskar R. Adsorption of basic red 9 onto activated carbon derived from immature cotton seeds: isotherm studies and error analysis. Desalination Water Treat. 2014 Dec 6;52(40–42):7743–65.

51. Ayawei N, Ebelegi AN, Wankasi D. Modelling and Interpretation of Adsorption Isotherms. J Chem. 2017 Sep 5;2017:e3039817.
52. Daifullah AAM, Girgis BS, Gad HMH. Utilization of agro-residues (rice husk) in small waste water treatment plans. Mater Lett. 2003;57(11):1723–31.
53. Abdelwahab O, Nemr A El, El-Sikaily A, Khaled A. Use of rice husk for adsorption of direct dyes from aqueous solution: A case study of direct F. Scarlet Green synthesis of TiO2 nanoparticles and its toxicity View project Industrial valorization of local biological materials and wastes for wastewater tre. Egypt J Aquat Res. 2005;31(May).
54. Della VP, Kühn I, Hotza D. Caracterização de cinza de casca de arroz para uso como matéria-prima na fabricação de refratários de sílica. Quimica Nova. 2001;24(6):778–82.